Scientia Africana, Vol. 22 (No. 2), August, 2023. Pp 177-202
© Faculty of Science, University of Port Harcourt, Printed in Nigeria *ISSN 1118 – 1931*

TEXTURAL CHARACTERISTICS AND SEDIMENT TRANSPORT DYNAMICS OF THE SANDSTONES OF THE NKPORO GROUP, SOUTHERN ANAMBRA BASIN (NIGERIA): EVIDENCE FOR THE UPPER CRETACEOUS SEA-LEVEL LOWSTAND

Ugwueze C.U. and Okengwu K.O.
Department of Geology, University of Port Harcourt, PMB 5323 Choba, Port Harcourt, Nigeria
Email: charles.ugwueze@uniport.edu.ng; +2348035632241

Received: 05-04-2023
Accepted: 30-07-2023

https://dx.doi.org/10.4314/sa.v22i2.17

Journal Homepage: http://www.scientia-african.uniportjournal.info
Publisher: *Faculty of Science, University of Port Harcourt.*

ABSTRACT

The Anambra sedimentary basin is one of the major inland basins in Nigeria. It covers an area of approximately 30,000 square kilometres and is named after the Anambra River, which traverses the basin. The geology of the basin is characterized by a complex sequence of sedimentary rocks that record a long history of deposition and tectonic activity. Detailed and systematic field investigation of its rock sequences exposed at Leru junction and adjoining localities revealed five dominant lithologic units consisting of massive sandstone facies, argillaceous sandstone facies, fissile black shale and mudstone facies, planar and ripple laminated sandstone facies, and massive and pebbly sandstone facies. The area is dominated by transgressive facies characterized by alternating sequences of thinly and parallel laminated fissile black shales, mudstones, and argillaceous sandstones overlain by regressive deposits dominated by massive and partly pebbly sandstones. The transgressive sequences perhaps represented shelf mud sedimentation that was probably interrupted by episodic influxes of sands rich in argillaceous materials transported down the shelf probably by shoreface waves or gravity-driven flows, while the regressive facies may have probably been emplaced by liquefied sand flows of the frontal slope of an advancing mouth bar. The erosion of the shelf deposits by the pebbly sandstones possibly reflected seaward migration of shallow distributary channels during sea-level low stand. Thus, facies transition from argillaceous sandstones to massive and pebbly sandstones within the continental shelf perhaps signified a fall in the relative sea level possibly triggered by the erosion of the shelf or perhaps a high rate of sediment supply.

Keywords: Textural Characteristics, Sediment Transport, Upper Cretaceous, Sandstones, Nkporo Group, Anambra Basin

INTRODUCTION

Textural analysis and study of sediment transport dynamics have increasingly become an important aspect of reservoir characterization; an aspect that essentially depends on the nature of the sediment source area, the mode of transport, the medium of transport, the energy of the transporting medium, and the distance of transport. Evaluating such clastic rocks entails not only the establishment of their grain sizes, the degree of sorting, their roundness, and grain/matrix ratios but also their textural and mineralogical maturities. Apart from proving

essential in the evaluation of reservoir potential, quality, and performance, textural analysis of clastic sediments characteristically aids in the determination of various transportation mechanisms that ancient sediments may have undergone in the course of their final deposition. There has been observable evidence, which shows that the size and sorting of sediment grains reflected sedimentation mechanisms and depositional conditions. However, grain size characteristics of sediments may show as much variability within different parts of the same environmental setting as between different environments (Boggs, 1987). Hence, reliability in the use of grain size techniques alone for identifying depositional environments of modern sediments becomes even more questionable when applied to ancient sedimentary rocks (Pettijohn, 1975 & Boggs, 1987).

The use of statistical moment for textural analysis has been employed by Folk and Ward (1957), and Friedman and Sanders (1978) among others. Friedman (1961 and 1979) popularised the use of two-component grain-size variation diagrams for environmental discrimination in which one statistical parameter (Mean Cubed Deviation) was discriminated against another (Moment Standard Deviation). Passega (1964) developed a different approach to environmental analysis whereby a grain diameter (C) corresponding to the first percentile (1%) on a cumulative curve was discriminated against the median diameter (M). Visher (1969) compared cumulative curves of grain-size data with the knowledge that cumulative log probability curves commonly do not plot as a single straight line but instead display two, three, or more straight-line segments in which each segment of the curve was interpreted to represent different transport modes by suspension, saltation or bed load transport.

Okoro (1995), Akaegbobi and Schmitt (1998), and Akaegbobi and Boboye (1999) through field study and laboratory analyses established that sandstone facies of the Nkporo Formation were generally fine to medium-grained, moderately sorted, texturally immature and mineralogically super mature quartz arenite. However, only a few studies have been able to apply an integrated approach involving the use of statistical moments of Folk and Ward (1957), Friedman and Sanders (1978), and the cumulative curves of grain-size data of Visher (1969) in the environmental analysis of the outcropping sandstone facies of the group. More so, the aspect of lithofacies analysis was barely incorporated into the evaluation of the depositional environments. Nevertheless, Akaegbobi *et al*. (1999) noted that the group represented the basal lithostratigraphic unit that unconformably overlies the pre-Santonian sediments of the Asu River Group and conformably overlain by the Mamu Formation. They characteristically assigned Campanian-Maastrichtian age to the group based on the occurrence of calcareous *Afrobolivina afra*, which suggested a shallow marine environment ranging from littoral to sub-littoral sub-environments.

LOCATION AND GEOLOGIC SETTING

The study area is located in the Isi-Ukwu Ato Local Government Area of Abia State, along the Enugu-Port Harcourt expressway (**Figures** 1a and 1b). It geographically lies between latitudes 5º54'N and 5º55'30''N, and longitudes 7º24'E and 7º25'E with an aerial extent of approximately thirteen square kilometres ($13km^2$) on a base map with a scale of 1: 12500 (**Figure** 1b).

Scientia Africana, Vol. 22 (No. 2), August, 2023. Pp 177-202
© Faculty of Science, University of Port Harcourt, Printed in Nigeria *ISSN 1118 – 1931*

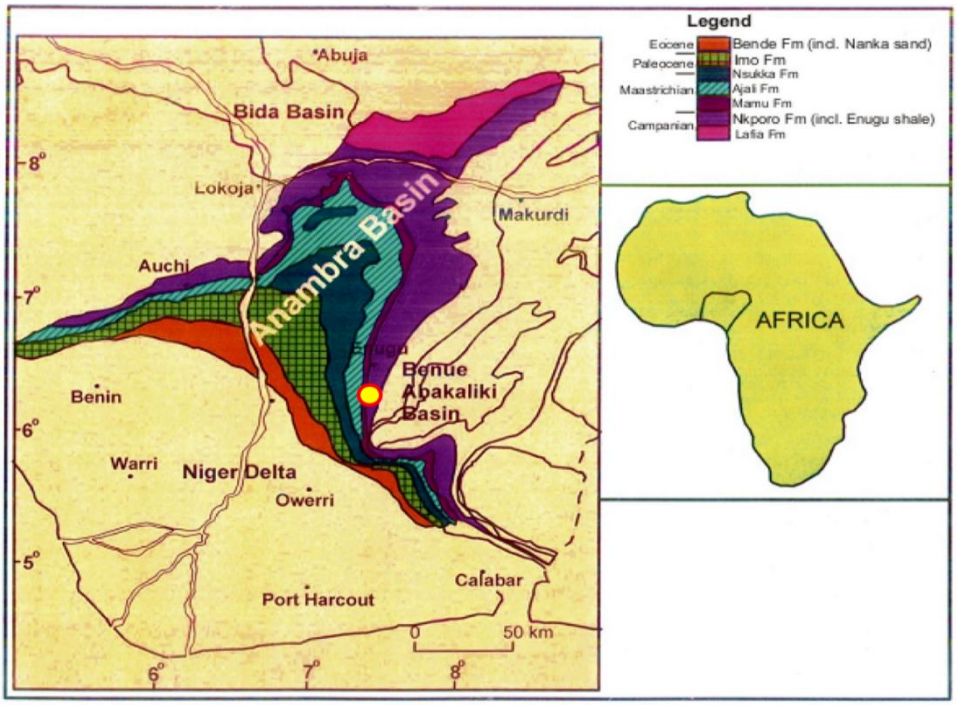

Fig. 1a: Geologic map of Nigeria, showing some stratigraphic units (e.g., Nkporo Formation, Mamu Formation, Ajali Sandstone, etc, and adjoining basins) and the location of the study area (highlighted in red circle). An inset is the map of Africa, showing the location of Nigeria (Source: Agoha *et al*., 2021)

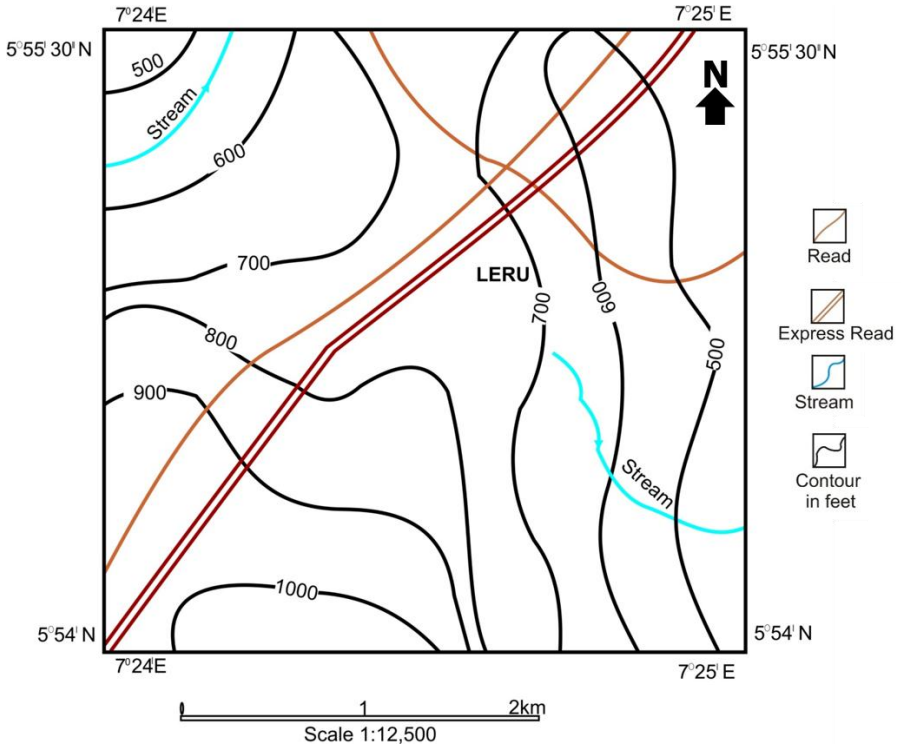

Fig. 1b: Topographic map of the study area, showing major roads and watersheds (See Figure **1a** above for the location of the study area marked in a red circle)

The tectonic framework of the continental margin along the west coast of Equatorial Guinea was controlled by the Cretaceous fracture zones expressed as trenches and ridges in the deep Atlantic. The fracture zone ridges subdivided the margin into individual basins, and in Nigeria, form the boundary faults of the Cretaceous Benue-Abakaliki Trough, which cut far into the West African Shield. The trough represents a failed arm of a rift, a triple junction, associated with the opening of the South Atlantic (**Figure** 2).

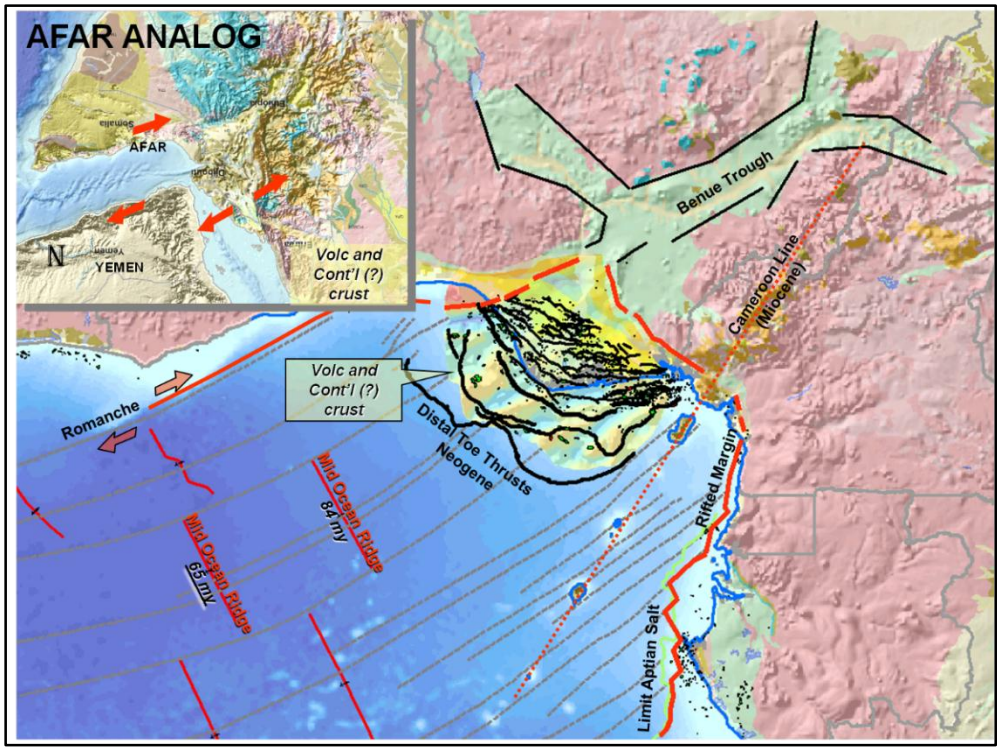

Fig. 2: Tectonic Framework of the Continental margin along the west coast of Equatorial Guinea, showing some fracture zone ridges and trenches in the deep Atlantic. An inset is the Afar Analog (modified from Ejedawe *et al.*, 2004)

In this region, rifting started in the Late Jurassic and persisted into the Middle Cretaceous (Burke *et al*, 1971; Burke, 1972; Burke and Whiteman, 1973). As the separation of the African and South American lithospheric plates got underway, spreading ridges and long–ridge–ridge transforms developed in the Gulf of Guinea; compressional stresses along the plate boundaries and incipient plate boundaries diminished bringing an end to the Santonian compressional phase. As the Santonian fold belt developed, the Anambra platform became a major depocenter (**Figure** 3) (Murat, 1972 & Ekwenye *et al.*, 2020).

The Anambra delta complex developed and by Palaeocene times had prograded onto the continental margin. Development of the complex was however terminated by the Imo Shale (Palaeocene) transgression (Whiteman, 1982). On the flanks of the fold belt, marginal basins such as the Anambra, Wukari–Mutum Biyu, and Wase Gombe basins formed, and on the newly developed continental margin, Dahomey, Ghana Offshore, Cameroun basins, and the Niger Delta complex evolved under a tensional regime (Whiteman, 1982).

Probably, contemporaneously with the development of the Abakaliki-Benue fold belt, the Anambra platform and associated

Scientia Africana, Vol. 22 (No. 2), August, 2023. Pp 177-202
© Faculty of Science, University of Port Harcourt, Printed in Nigeria *ISSN 1118 – 1931*

elements, which had been gently subsiding units since medial Albian times (**Figure** 3), subsided even more and the regional axis of deposition which hitherto had been centred in the Abakaliki Trough shifted westwards (**Figures** 3 and 4) (Murat, 1972 and Whiteman, 1982 & Ekwenye *et al.*, 2020).

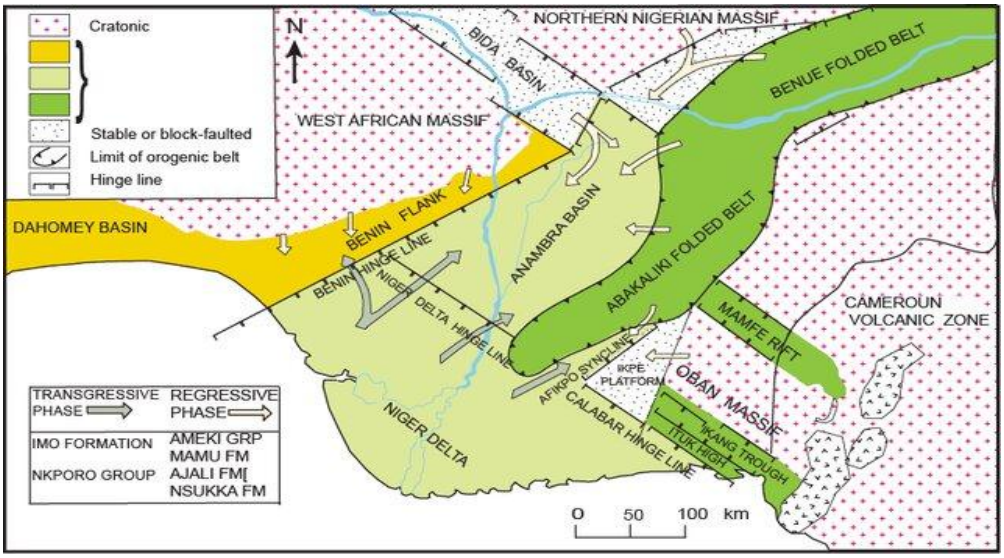

Fig: 3: Tectonic Map of South-Eastern Nigeria during the Albian to Lower Santonian times, showing some depositional axes such as the Anambra Platform and the Abakaliki Trough (Source: Ekwenye *et al.*, 2020)

The Anambra basin appears to have been boarded on the northwest by the Benin flank consisting mainly of basement complex rocks and to have been joined at its northern end to the middle Niger embayment (Burke *et al*, 1973). On the southeast, the basin is bounded by the Abakaliki fold belt. The basin is bounded on the southwestern flank by the Niger Delta hinge line developed in relation to the old ridge-transform break between South America and Africa.

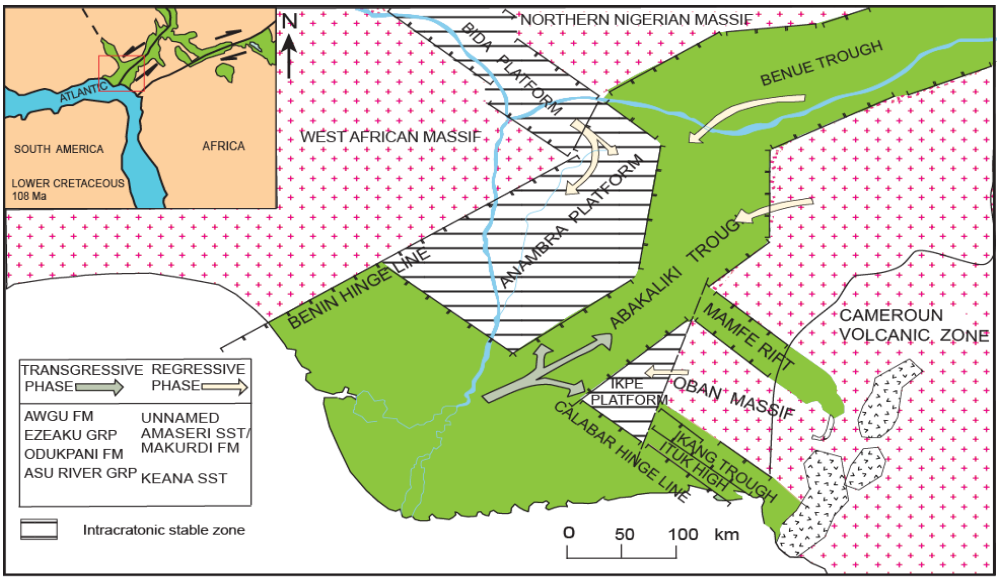

Fig: 4. Tectonic Map of South-Eastern Nigeria during the Campanian to Eocene time, showing some depositional axes such as the Anambra Platform and the Abakaliki Trough (Source: Ekwenye *et al.*, 2020)

The stratigraphic succession in the Anambra basin had been reviewed by Murat (1972), Reyment (1965), Agagu *et al.,* (1983), Ladipo (1988) and Oladotun *et al.,* (2016) among others. They divided the basin into four formations with their lateral equivalents. These lithostratigraphic units consist of the basal Nkporo Shale, Mamu Formation, Ajali Sandstone, and Nsukka Formation. The post-Santonian successions in the basin began with the basal marine Nkporo Shale (**Figure** 5), which had been dated as Late Campanian by Zaborski (1983) based on ammonites, *Libycoceras dandense* and *Bostrychoceras palyplochum*, and Campanian-Maastrichtian age by Akaegbobi *et al.,* (1999) based on the occurrence of calcareous *Afrobolivina afra*.

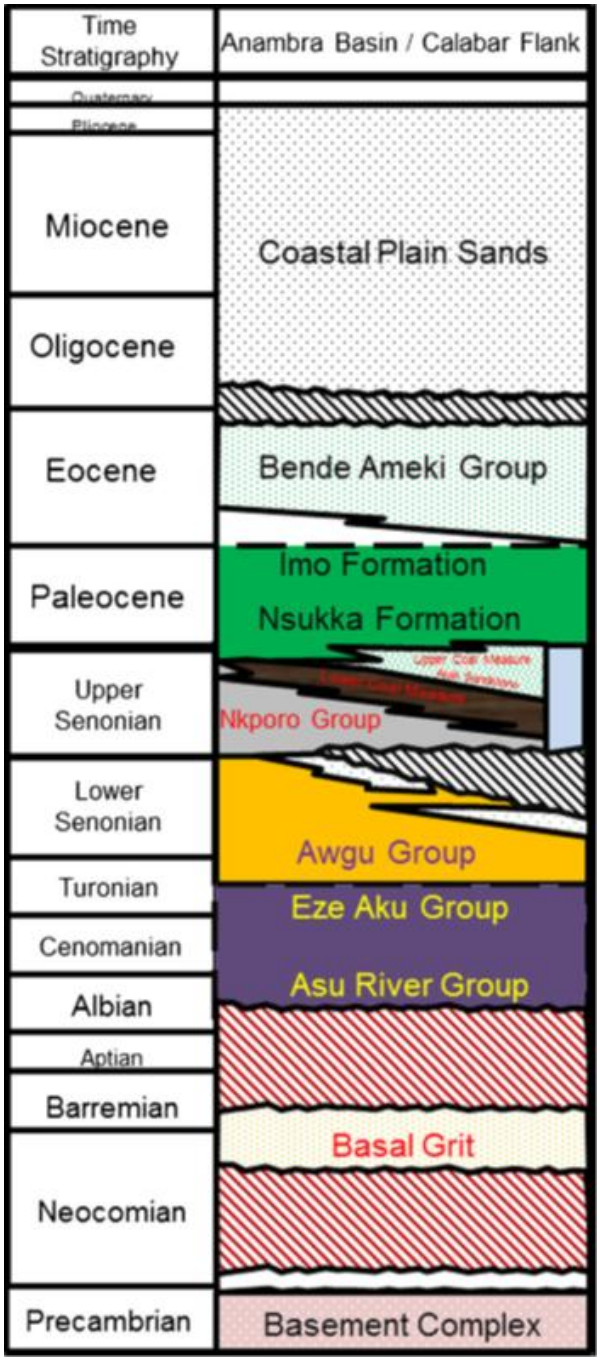

Fig: 5. Stratigraphic Section of the Anambra Basin, showing the stratigraphic position of the Nkporo Shale (Source: Oladotun *et al.,* 2016)

Scientia Africana, Vol. 22 (No. 2), August, 2023. Pp 177-202
© Faculty of Science, University of Port Harcourt, Printed in Nigeria *ISSN 1118 – 1931*

MATERIALS AND SAMPLING TECHNIQUES

The database for this study was generated using a topographic map (**Figure** 1b), compass clinometer, GPS Garmin Map76 (**Table** 1), field notebook, handheld magnifying lens, masking tape, sample bags, geologic hammer, measuring tape, Jacob's stick, grain size comparator, roundness chart, marker, dilute hydrochloric acid and 2HB pencil. The field procedure involved outcrop description, measurements, and sample collection.

Desktop research including an examination of the geologic map sheet (Sheet-79) of Umuahia was carried out prior to the commencement of the field mapping to possibly identify and delineate outcrop trends, geologic formations, watershed, possible routes to outcrops, and some landmarks. Description of outcrop exposures including rock types, bed thicknesses, lithologic boundaries, strikes and dips, rock colours, grain sizes, grain shapes, and grain sorting were essentially carried out where necessarily possible from the base to the top of each outcrop section visited. The sedimentological descriptions involved facies analysis and environmental interpretations. Sketches of stratal profiles were also made at different outcrop locations visited while photographs were taken of rock exposures with interesting geologic features. Representative fresh sandstone samples were collected across strikes of beds and properly labelled for onward laboratory analysis.

Table 1: Measurements of Latitudes and Longitudes of the sample locations using GPS Garmin Map76

Stops	Northings	Eastings	Elevation (m)	Accuracy (m)
1	05^0 55.150′	07^0 24.692′	202.4	±10.9
2	05^0 55.098′	07^0 24.610′	212.6	±19.4
3	05^0 55.075′	07^0 24.598′	202.5	±27.3
4	05^0 55.055′	07^0 24.581′	215.5	54.5
5	05^0 54.996′	07^0 24.546′	218.9	±15.7
6	05^0 55.002′	07^0 24.533′	214.2	±17.1
7	05^0 54.969′	07^0 24.516′	213.4	±9.8
8	05^0 54.853′	07^0 24.434′	203.5	±7.8
10	05^0 54.803′	07^0 24.382′	207.1	±8.2
11	05^0 54.780′	07^0 24.382′	213.7	±8.8
12	05^0 54.522′	07^0 24.099′	219.7	±23.9
13	05^0 55.223′	07^0 24.697′	201.2	±24.5

Data Analysis Techniques

Fifteen sandstone samples collected across the study area amenable to disaggregation (Okoro, 1995) and weighing 50 grams each were sieved using a sieve nest of one phi interval (ASTM) on a Pascal automatic shaker for 15 minutes. The weights retained were corrected for sieve loss before their successive conversion to weight percent. The successive summations in descending order of the weight percent gave the cumulative weight percent (**Table**s 2a-c).

The histograms (**Figures** 6a-c) were derived by plotting the values of the weight percent along the y-axis against the values of grain diameter (phi-scale) along the x-axis while the

cumulative log probability curves (**Figures** 7a-c) were obtained by plotting the cumulative weight percent on the y-axis against the grain diameter (mm) along the x-axis. The slope of the lines was a function of the standard deviation of the distribution.

Statistical parameters, a textural descriptor, of the grain size distributions, were derived using the moment method as recommended by Krumbein and Pettijohn (1938). The entire sets of the statistical moment were computed as shown in Tables **(**3a-c). The diameter classes (**Φ**) were placed in the first column, the midpoint ($\mathbf{X_1}$) in the second column and the frequency (**f**) of the weight per cent in the third. The Midpoint of the grain diameter with the highest occurrence ($\mathbf{X_0}$) was determined for each data set representing various locations sampled. The '**d**' scale was calculated as shown in column four (**Tables** 3a-c). Subsequent scales such as '**fd**', '$\mathbf{d^2}$', '$\mathbf{fd^2}$', '$\mathbf{d^3}$', '$\mathbf{fd^3}$', '$\mathbf{d^4}$', and '$\mathbf{fd^4}$' were calculated also as shown in the various columns.

The moments; $\mathbf{n_1}$, $\mathbf{n_2}$, $\mathbf{n_3}$, and $\mathbf{n_4}$ moments about the '**d**' origin were calculated by dividing the algebraic totals of the products ('**fd**', '$\mathbf{fd^2}$', '$\mathbf{fd^3}$' and '$\mathbf{fd^4}$') in the various columns by 100 (see, **Figures** 3a-c). The various **n**-values were substituted accordingly in the equations for each of the moment measures according to Friedman and Sanders (1978) (**Table**: 4), while interpretation of the results of the various moment measures was done using the verbal terms and interpretation of Folk and Ward (1957) (**Table**: 5). Various bivariate analyses were undertaken following the works of Friedman (1961), Passega (1964), Visher (1969) and Friedman (1979).

Table: 4: Equations for Moment Calculations (Source: Friedman and Sanders, 1978)

Parameters	**Formular**	
First Moment	$\mathbf{M_\Phi = X_0 + n_1}$	***equ. 1***
Second Moment	$\mathbf{\delta_\Phi = \sqrt{n_2 - (n_1)^2}}$	***equ. 2***
Third Moment	$\mathbf{S_{K\Phi} = M_3 / 2\delta^3_\Phi}$ $(M_3 = n_3 - 3n^2n_1 + 2n_1^3)$	***equ. 3***
Fourth Moment	$\mathbf{K_\Phi = \beta_2 - 3;}$ $(\beta_2 = M_4 / \delta^4_\Phi)$ $(M_4 = n_4 - 4n_1n_3 + 6n_1^2n_2 - 3n_1^4)$	***equ. 4***

(See **Tables** 3a-c for the interpretation of X_0, n_1, n_2, n_3, n_4)

Table: 5: Verbal Terms and Interpretation (Source: Folk and Ward, 1957)

Parameters	**Verbal Terms and Interpretation**
FIRST MOMENT	0 to 1: Coarse Sand 1 to 2: Medium Sand 2 to 3: Fine Sand
SECOND MOMENT	< 0.35: Very Well Sorted 0.35 to 0.50: Well Sorted 0.50 to 0.71: Moderately Well Sorted 0.71 to 1.0: Moderately Sorted 1.0 to 2.0: Poorly Sorted 2.0 to 4.0: Very Poorly Sorted > 4.0: Extremely Poorly Sorted
THIRD MOMENT	> 0.30: Very Positively Skewed 0.3 to 0.1: Positively Skewed 0.1 to -0.1: Near Symmetrical

Scientia Africana, Vol. 22 (No. 2), August, 2023. Pp 177-202
© Faculty of Science, University of Port Harcourt, Printed in Nigeria *ISSN 1118 – 1931*

	-0.1 to -0.3: Negatively Skewed
	< -0.3: Very Negatively Skewed
FOURTH MOMENT	< 0.67: Very Platykurtic
	0.67 to 0.90: Platykurtic
	0.90 to 1.11: Mesokurtic
	1.11 to 1.50: Leptokurtic
	1.50 to 3.0: Very Leptokurtic
	> 3.0: Extremely Leptokurtic

RESULTS

Lithofacies Analysis

Detailed and systematic field investigations of the sedimentary rocks exposed at the Leru junction and adjoining localities revealed five dominant lithologic units consisting of massive sandstones, argillaceous sandstones, fissile black shales and mudstones, planar and ripple laminated sandstones, and pebbly sandstones. The strata were nearly flat-lying, and gently dip at an angle of less than 6˚NW while striking between 40˚ to 50˚NE.

a) Massive Sandstones

The massive sandstones appeared un-bedded or very thickly bedded, structureless, coarse to medium-grained, and poorly to moderately sorted in texture. Where sedimentary structures were present, they appeared faint, comprising large dish structures and dewatering chutes (**Plates 1**, 2, and 3, and **Figure** 8). The massive coarse-grained sandstones were bioturbated by vertically and horizontally branching *Ophiomorpha* burrows. The unit was common in the northwest section of the study area. The sequence was overlain by 40cm thick bioturbated micaceous whitish sandstones followed by 20cm thick pinkish medium-grained sandstones overlain by more than 40cm thick and thinly laminated dark grey shales.

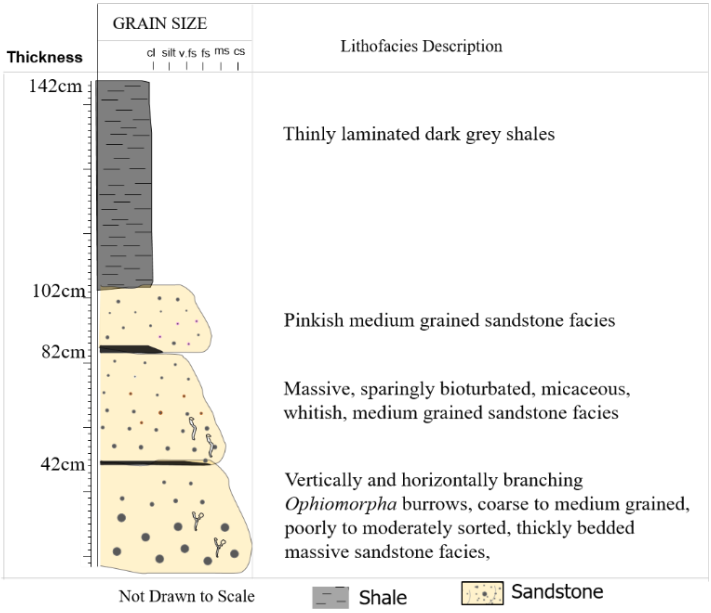

Fig: 8: Stratal log profile of the massive sandstone outcropping in the north-western part of the study area, showing various lithological successions

b) Argillaceous Sandstones

The argillaceous sandstones were ungraded, calcareous, and poorly sorted with a high percentage of mud fractions in the matrix, which gave them dirty appearances. Occasionally, small-scale sub-angular pebbles of quartz occurred scattered within the facies. The unit occasionally comprised planar cross bed sets overlying weathered shales (**Plates**: 4 and 5, and **Figure** 9) outcropping in the north-western section of the study area. The argillaceous sandstones and the massive coarse-grained sandstones could be laterally traced onto one another. The cross-bedded argillaceous sandstones prograded from the north-western part and inter-fingered with the massive coarse-grained sandstones down northeast into a weathered shale sequence.

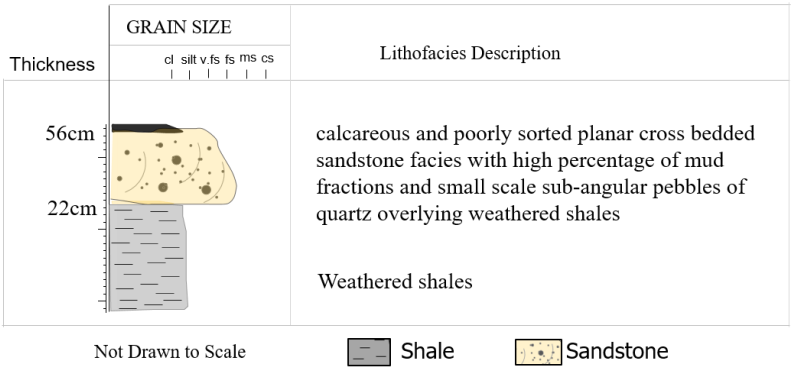

Fig: 9: Stratal log profile of the argillaceous sandstone sequence underlain by the weathered shales

c) Fissile Black Shale and Mudstones

Further, down east of the north-western part (central portion) of the study area, weathered shales and mudstones totally predominated over sandstones. The inter-bedded sequence consisted of muddy shales at the base overlain by over 34cm thick ferruginized shales. The lithologic successions were subsequently overlain by over 20cm thick mudstones followed by more than 60cm thick iron-stained black shales with thin lamination. This was overlain by more than 35cm thick massive mudstones. The mudstone sequence was overlain by 250cm thick fissile black shales followed by another 15cm thick mudstone and an overburden cover (**Plates:** 6, 7, and 8; and **Figure** 10). Sharp and scoured contacts existed between beds. The fissility of the shales decreased laterally southwards of the study area and became more jointed with well-pronounced parallel lamination in the southwest. The thickness of the individual lamina increased relatively laterally southwards and became clayey within the central portion (**Plate:** 9).

Scientia Africana, Vol. 22 (No. 2), August, 2023. Pp 177-202
© Faculty of Science, University of Port Harcourt, Printed in Nigeria *ISSN 1118 – 1931*

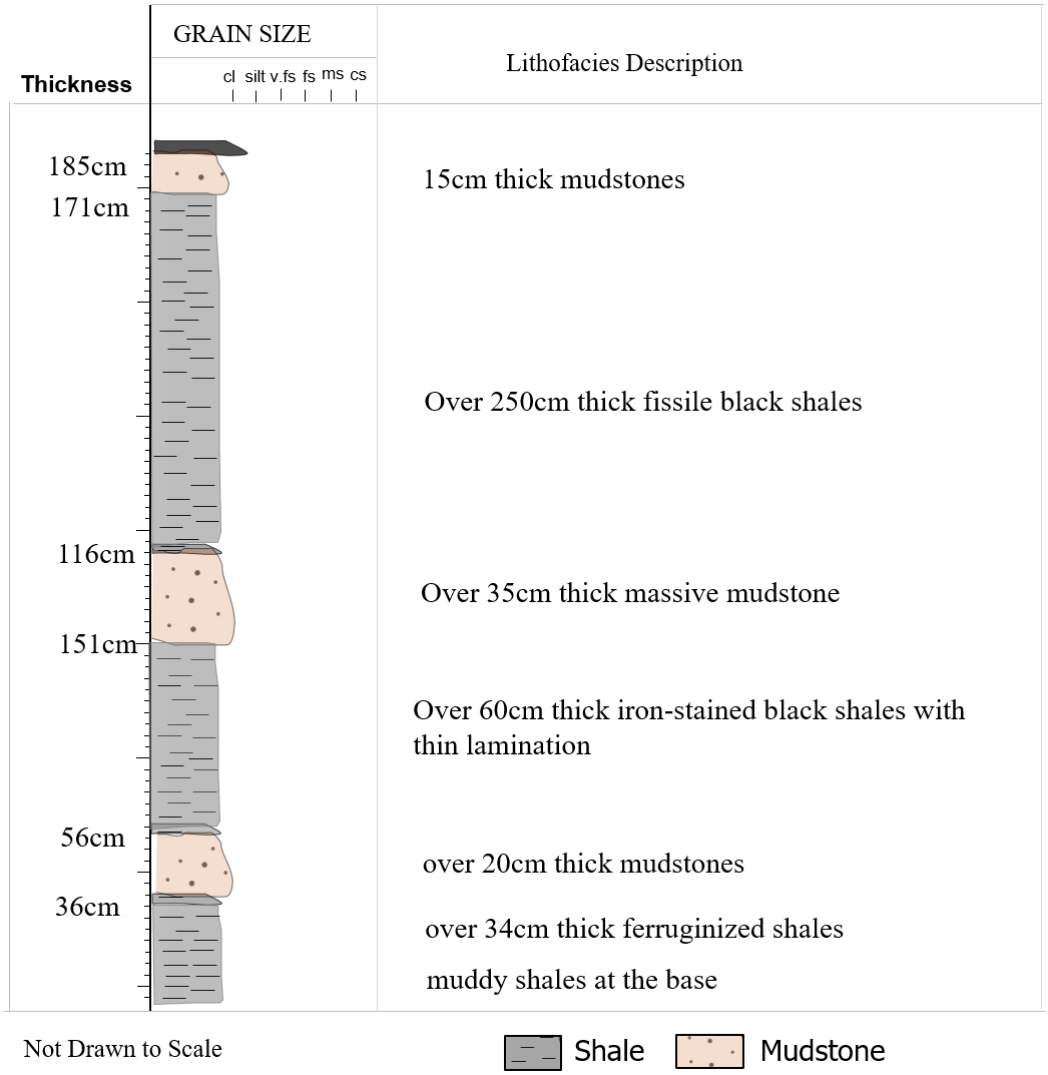

Fig: 10: Stratal log profile of the fissile black shale and mudstone sequence

d) Planar and Ripple Laminated Sandstones

In the southwest section of the study area, sandstones became dominant over shales once again with the total disappearance of mud rock. The sandstones commonly displayed planar and ripple laminations. Planar lamination was usually transitional upwards into current ripple lamination and occasionally into hummocky cross lamination (**Plates:** 11 and 12, and **Figure** 11). Southeast of the area, thicker beds commonly contained a structureless basal portion of sandstones overlain by planar laminated medium to coarse-grained sandstones (**Plates:** 13 and 14).

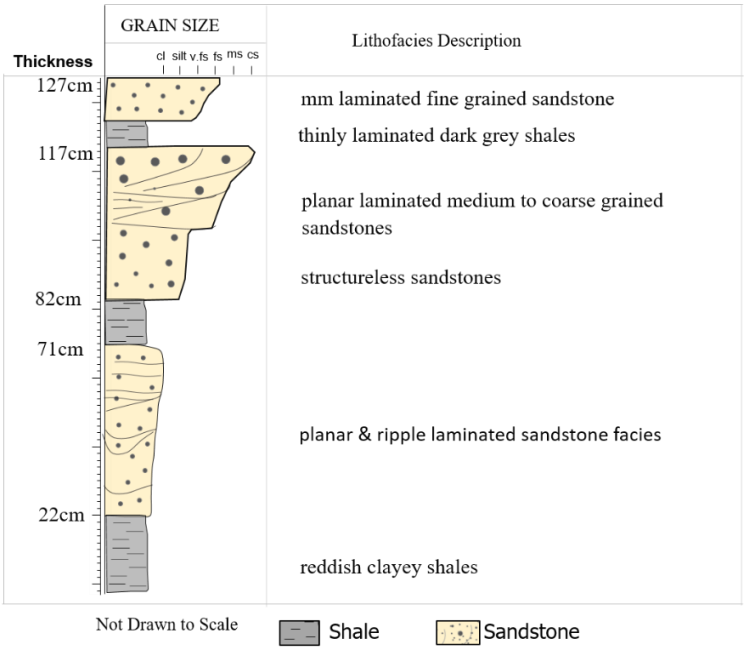

Fig: 11: Stratal log profile of planar and ripple cross-laminated sandstones

e) Parallel Laminated Shales

Parallel laminated shales occurred as basal units both in the southwest and northwest of the study area. The thickness of individual lamina increased south-westward (**Plate**: 15) compared to that outcropping in the north-western part (**Plate**: 16). In the far northwest, the lithofacies consisted of an alternating sequence of thinly bedded and parallel laminated 60cm thick basal black shales overlain by 30cm thick horizontally burrowed sandstones, followed by 70cm thick medium-grained and massive sandstones (**Plate:** 16 and **Figure** 12).

Fig: 12: Stratal log profile of the parallel laminated shales overlain by the planar bedded argillaceous sandstones **NW** of the study area

Scientia Africana, Vol. 22 (No. 2), August, 2023. Pp 177-202
© Faculty of Science, University of Port Harcourt, Printed in Nigeria *ISSN 1118 – 1931*

f) Massive and Pebbly Sandstones

In the northeast of the study area, the facies succession consisted of an alternating sequence of vertically burrowed, weathered 60cm thick pebbly and massive sandstones overlain by 12cm thick massive sandstones riddled with rib joints and lots of micaceous grains (**Plates:** 17 and 18).

Univariate Analysis

a) Particle Size Distribution Using Statistical Moments

The values of the grain diameter (**first moment**) ranged from (0.77) to (2.5) in the southwest of the study area with an average value of (1.5), and from (0.34) to (1.57) in the north with an average value of (1.14) displaying mostly medium to sub-ordinate coarse-grained character.

The values of the standard deviation (**second moment**) ranged from (0.9) to (1.8) in the southwest of the study area with an average value of (1.25), and from (0.73) to (1.1) in the north with an average value of (0.89) indicating that the sandstones were generally poorly sorted in the southwest and moderately sorted in the north.

The values of the skewness (**third moment**) ranged from (-0.67) to (0.19) in the southwest with an average value of (-0.17) and from (-0.34) to (0.28) in the north with an average value of (-0.1) indicating that in the southwest, the sandstones were mostly very negatively to positively skewed with an average value of negative skewness. In the north, however, the sandstones were mostly near-symmetrical with an average value of also negative skewness.

The values of the kurtosis (**fourth moment**) ranged from (-0.83) to (1.07) in the southwest with an average value of (0.09), and from (-0.39) to (4.3) in the north with an average value of (1.5) indicating that the sandstones in the southwest were mostly very platykurtic while those from the northern part of the study area were mostly leptokurtic. The results of the grain size analysis performed on fifteen sandstone samples amenable to disaggregation are summarized in Table 5.

Table 5: Summary of the Textural Characteristics of the Sandstone Facies in the Study Area

LOCATION	STOP	FIRST MOMENT	SECOND MOMENT	THIRD MOMENT	FOURTH MOMENT
LERU SOUTH WEST 1	**12A**	2.5 Fine Sands	1.3 Poorly Sorted	-0.67 Very Negatively Skewed	1.07 Mesokurtic
		0.77 Coarse Sands	1.1 Poorly Sorted	0.19 Positively Skewed	0.01 Very Platykurtic
		1.3 Medium Sands	0.9 Moderately sorted	-0.18 Negatively Skewed	0.27 Very Platykurtic
LERU SOUTH WEST 2	**12B**	0.81 Coarse Sands	0.92 Moderately Sorted	0.12 Positively Skewed	0.28 Very Platykurtic
		2.1 Fine Sands	1.8 Poorly Sorted	-0.36 V. Negatively Skewed	-0.83 Very Platykurtic
AVERAGE		**1.5** **Medium Sand**	**1.25** **poorly sorted**	**-0.17** **Negatively Skewed**	**0.09** **Very platykurtic**
LERU NORTH WEST	**13A**	1.57 Medium Sands	0.75 Moderately Sorted	-0.34 Very Negatively Skewed	4.3 Extremely Leptokurtic
		1.2 Medium Sands	1.1 Poorly Sorted	-0.42 Very Negatively Skewed	1.06 Mesokurtic
		0.77 Coarse Sands	0.95 Moderately Sorted	0.02 Near Symmetrical	0.98 Mesokurtic
	13B	1.2 Medium Sands	1.04 Poorly Sorted	-0.1 Near Symmetrical	-0.39 Very Platykurtic
		0.35 Coarse Sands	1 Poorly Sorted	0.28 Positively Skewed	0.67 Platykurtic

		1.2 Medium Sands	0.73 Moderately Sorted	0.18 Positively Skewed	1.32 Leptokurtic
		1.2 Medium Sands	0.76 Moderately Sorted	-0.14 Near Symmetrical	1.3 Leptokurtic
AVERAGE		**1.07** **Medium Sands**	**0.9** **Moderately Sorted**	**-0.07** **Near Symmetrical**	**1.32** **Leptokurtic**
LERU NORTH EAST	**14A**	1.1 Medium Sands	0.89 Moderately Sorted	0.04 Near Symmetrical	1.56 Very Leptokurtic
		1.1 Medium Sands	0.8 Moderately Sorted	0.02 Near Symmetrical	0.49 Very Platykurtic
	14B	0.34 Coarse Sands	0.85 Moderately Sorted	0.23 Positively Skewed	2.06 Very Leptokurtic
AVERAGE		**0.85** **Coarse Sand**	**0.85** **Moderately Sorted**	**0.1** **Positively Skewed**	**1.37** **Leptokurtic**

Bivariate Analysis

a) Mean Cubed Deviation (MCD) versus Standard Deviation (MSD)

The use of two-component grain-size variation diagrams, in which one statistical parameter is plotted against another was popularized by Friedman (1961 and 1979). By plotting large numbers of grain-size analysis data of modern sediments on such diagrams, he drew a line separating the diagrams into major environmental fields.

This graphical technique has been used to characterize and differentiate the outcropping sandstone units in the study area into river and beach sediments. About 55% of the sands plotted into the one-way flow channels of the river while less than 45% plotted into the two-way flow channels of the beach thus indicating a depositional setting dominated more by fluvial than beach systems (**Figure** 13).

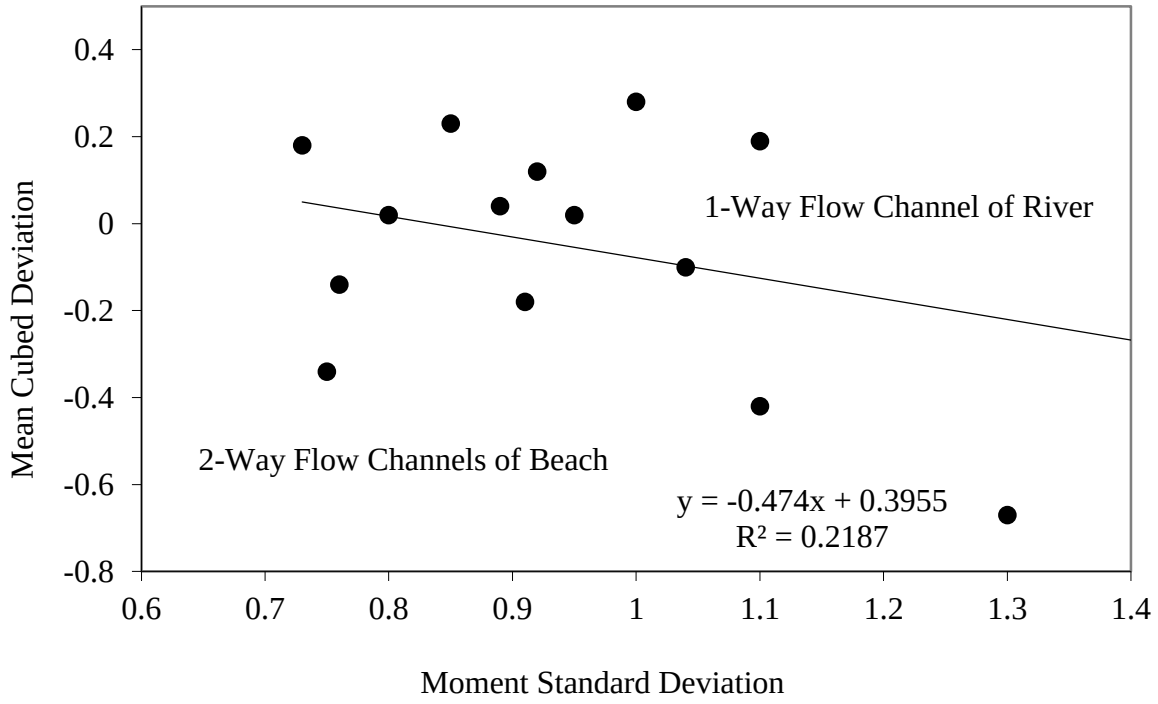

Fig. 13: Graph of Mean Cubed Deviation (MCD) versus Moment Standard Deviation (MSD) of the outcropping sandstones in the study area, showing the one-way flow channel of the river and the two-way flow channel of the beach (Source: Friedman, 1979)

Scientia Africana, Vol. 22 (No. 2), August, 2023. Pp 177-202
© Faculty of Science, University of Port Harcourt, Printed in Nigeria *ISSN 1118 – 1931*

b) First Percentile (C) **Versus Median Grain Diameter** (M)

Passega (1964) developed a different graphical approach to environmental analysis using two textural properties of grain size distributions namely the grain diameter (C) corresponding to the first percentile (1%) on the cumulative curve which measures the coarsest grains in a deposit, and the median grain diameter (M).

The first percentile values read from the various cumulative log probability curves (**Figures** 7a-c) ranged from 1200 to approximately 4600 microns while the median diameter values ranged from 125 to 650 microns (**Figure** 14). When plotted on the C-M diagram of Passega (1964), the results indicated that the sandstones were mainly fluvial deposits resulting from saltation and minor suspension transports.

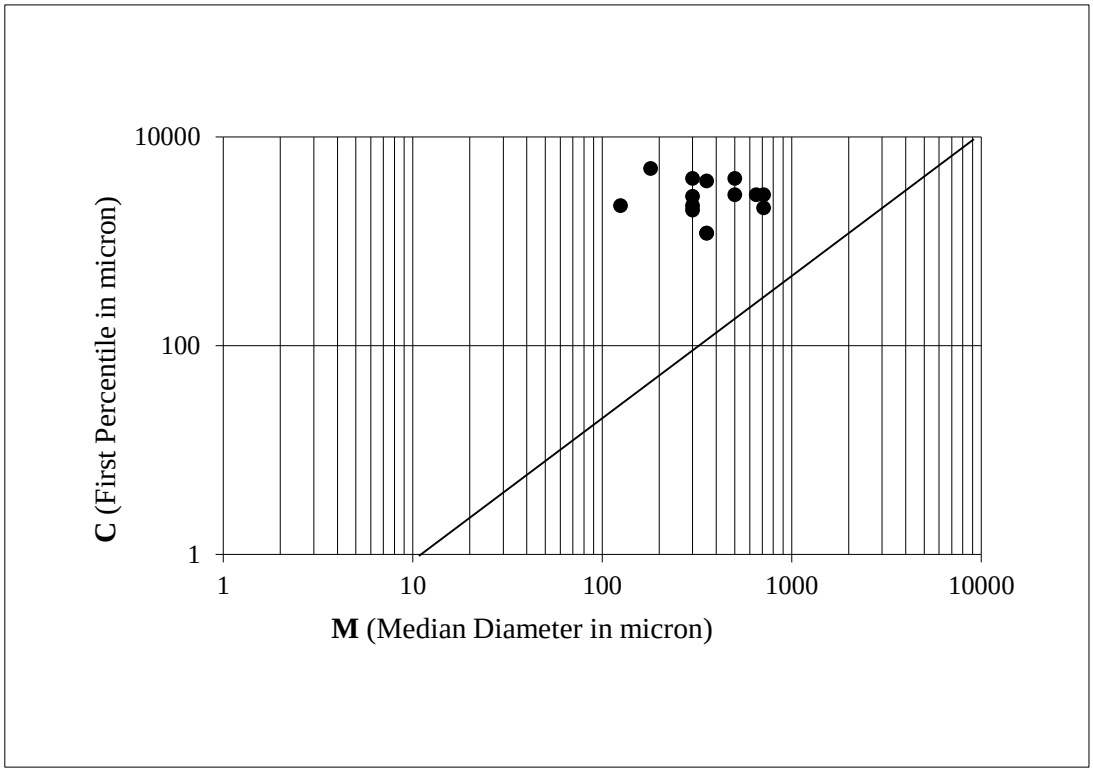

Fig. 14: Graph of the first percentile against the median diameter of the outcropping sandstone units in the study area (Modified after Passega, 1964)

c) Log Probability Curves

The third approach to environmental discrimination involved the comparison of cumulative curves of grain size data plotted on log probability paper (Visher, 1969) with the knowledge that cumulative log probability curves commonly do not plot as a single straight line but instead two, three, or more straight-line segments. Each segment of the curve was interpreted to represent different transport modes either by suspension, saltation, or bed load transport (**Figures** 7a-c). The log probability curves had saltation populations greater than 80% with coarse truncation points mostly at -2Φ to -1Φ, and suspension populations less than 10% with fine truncation points greater than 3Φ (**Figures** 7a-c). The cumulative log probability curves also displayed gentle to very gentle slopes.

DISCUSSION AND CONCEPTUAL GEOLOGICAL FRAMEWORK OF THE STUDY AREA

The influence of paleo morphology and paleocirculation pattern (Reijer *et al*., 1997), base-level changes (Ugwueze, *et al*., 2019), and frequent incursions of the sea during the Campanian-Eocene epoch in the Cretaceous period perhaps played a major role in the reconstruction of the conceptual geological framework of the southern Anambra basin (**Figure** 15). Detailed and systematic field investigation of the sedimentary rocks exposed at Leru junction and the adjoining localities revealed five dominant lithologic units from which the geological framework of the area was reconstructed. These lithologic units consist of massive sandstones, argillaceous sandstones, fissile black shales, mudstones, planar and ripple laminated sandstones, and massive and pebbly sandstones (**Plates** 1-18).

Within the central section of the study area, transgressive facies were characterized by alternating sequences of thinly and parallel laminated fissile black shales, mudstones, and argillaceous sandstones that were dominated by regressive deposits. The sequences perhaps represented shelf mud sedimentation that was probably interrupted by episodic influxes of sands rich in argillaceous materials transported down the shelf probably by shoreface waves or gravity-driven flows. Argillaceous sandstones have been reported from lots of depositional settings cutting across river deltas, shoreface, storm deposits, sand waves, offshore bars, turbidites, tidal deltas, and flats (Chris *et al*., 2017 and Ugwueze *et al*., 2019).

The general upward transition from the alternating sequences of thinly and parallel laminated fissile black shales, mudstones, and argillaceous sandstones into the massive and partly pebbly sandstones is interpreted as reflecting an increasing energy condition of deposition brought about by perhaps channel avulsion or a reflection of supply of very highly concentrated sedimentary detritus. Thus, the argillaceous sandstones probably marked the beginning of a prograding delta over shallow water shelf deposits (Sinclair, 1993; Okoro, 1995; Reijers *et al*., 1997, and Ugwueze *et al*., 2019).

The structureless mudstones showed no obvious lamination or fissility irrespective of the weathering stage, instead, they showed block fracture patterns and may just be massive and homogeneous. Nevertheless, the absence of obvious lamination in the sandstones may be due to a lack of original depositional layering, which may be an indication of rapid deposition from suspension or may have resulted from very highly concentrated sediment dispersions during sediment gravity flow or later destruction of layering.

The massive sandstones may have probably been emplaced by liquefied sand flows of the frontal slope of an advancing mouth bar. The erosion of the shelf deposits by pebbly sandstones possibly reflected seaward migration of shallow distributary channels during sea level low-stand.

Scientia Africana, Vol. 22 (No. 2), August, 2023. Pp 177-202
© Faculty of Science, University of Port Harcourt, Printed in Nigeria *ISSN 1118 – 1931*

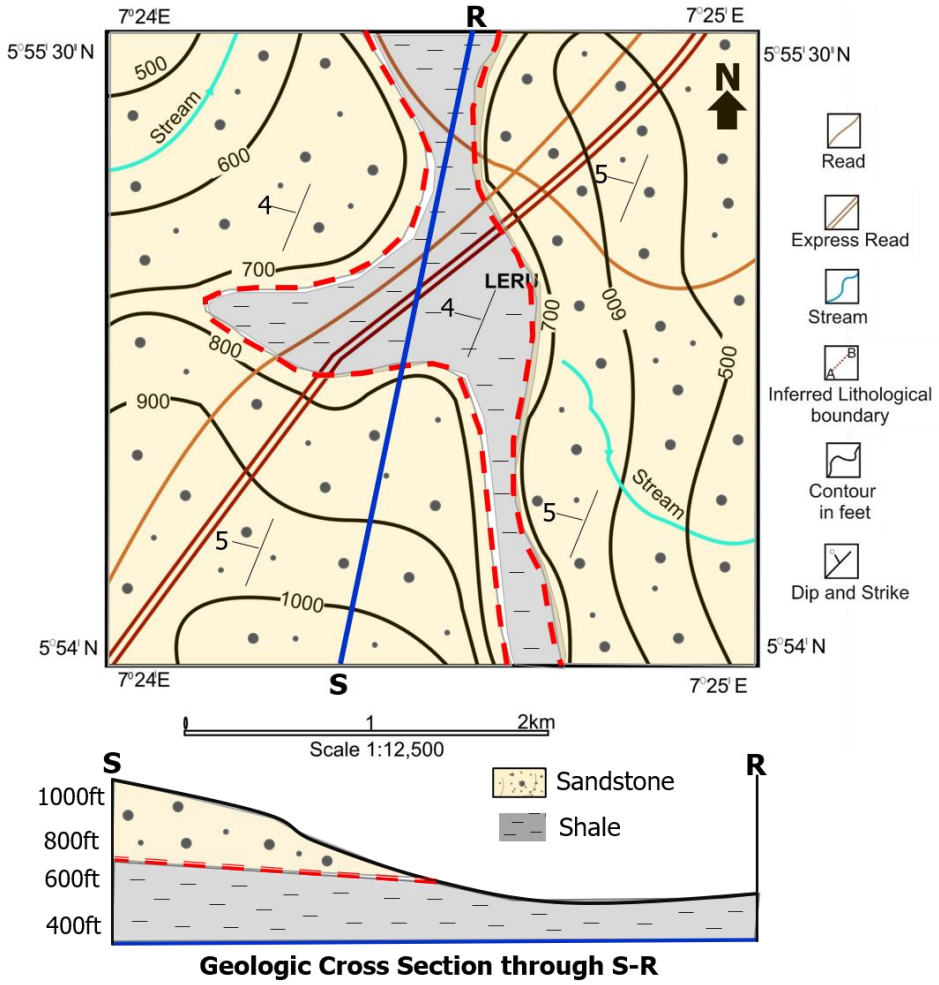

Fig. 15: Geological map of Leru section and adjoining areas, showing various lithologic units and their cross-sectional view from S-R

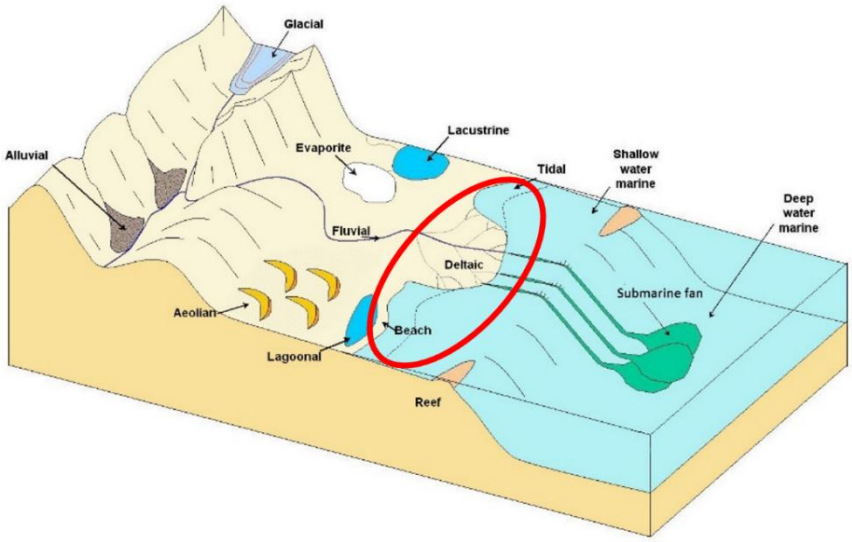

Fig. 16: Prograding shoreface to delta front conceptual depositional model of the sandstone facies outcropping at Leru section and environs. Circled in red is the position of the shallow water shelf comprising the prograding delta front and shoreface environments (modified from Chris *et al*., 2017 and Ugwueze, *et al*., 2019)

CONCLUSION

The area is dominated by transgressive facies characterized by alternating sequences of thinly and parallel laminated fissile black shales, mudstones, and argillaceous sandstones overlain by regressive deposits dominated by massive and partly pebbly sandstones. The transgressive sequence perhaps represented shelf mud sedimentation that was probably interrupted by episodic influxes of sands rich in argillaceous materials transported down the shelf probably by shoreface waves or gravity-driven flows while the regressive facies may have been emplaced by liquefied sand flows of the frontal slope of an advancing mouth bar. Erosion of the shelf deposits by the pebbly sandstones possibly reflected seaward migration of shallow distributary channels during sea level low-stand. Thus, the facies transition from argillaceous sandstones to massive and pebbly sandstones within the continental shelf perhaps signified a fall in the relative sea level that was possibly triggered by the erosion of the shelf or a high rate of sediment supply.

REFERENCES

Agagu, O. K. & C.I. Adigbije (1983). Tectonic sedimentation framework of Lower Benue Trough, Southern Nigeria. *Journal of African Earth Science*, 1, 267-274.

Agoha, C.C., Mgbeojedo, T.I., Okoro, E.M., Akiang, F.B., Onwubuariri, C.N. & L.S. Al-Naimi (2021). Geologic mapping and basement–sediment contact delineation along Profile X, Igarra–Auchi area, Southern Nigeria using ground magnetic and electromagnetic methods. *Journal of Petroleum Exploration and Production Technology*, 11, 2519–2537

Akaegbobi, I. M., & M. Schmitt (1998). Organic facies, Hydrocarbon source potential, and the reconstruction of the depositional paleoenvironment of the Campano-Maastrichtian Nkporo Shale in the Cretaceous Anambra Basin, Nigeria. *Nigerian Association of Petroleum Explorationists* Bulletin, 13(1) 1-19.

Akaegbobi, I. M., & O.A. Bobye (1999). Textural, Structural Features, and Microfossil Assemblage Relationship as delineating Criteria for the Stratigraphic Boundary between Mamu Formation and Nkporo Shale within the Anambra Basin Nigeria. *Nigerian Association of Petroleum Explorationists* Bulletin, 14(2) 193-208.

Boggs, S. J., 1987. Principles of Sedimentology and Stratigraphy. Macmillan Publisher New York, 784P.

Burke, K. C. (1972). Longshore drift, submarine canyons, and submarine fans in the development of the Niger Delta. *American Association of Petroleum Geologists* Bulletin, 56, 1975-1983.

Burke, K. C.; Dessauvagie, T. F. W., A.J. Whiteman (1971). Opening of the Gulf of Guinea, and geological history of the Benue Depression and Niger Delta Nature. *Physical Science*, 233, 51-55.

Burke, K. C. & A.J. Whiteman (1973). Uplift, rifting and the breakup of Africa: In Tarling, D. H., Runcon, S. K. (eds.), Implications of continental drift to Earth Sciences. Academy Press London, 735-755.

Chris, J., Matthew, D.A., Paul, I., & M. Cam (2017). An Introduction to Geology: Free Textbook for College-Level Introductory Geology Courses, Salt Lake Community College. Retrieved April 05, 2023, from https://opengeology.org/textbook/

Ejedawe, J.E; Lehner, B.L; Meyer, S.; Olugbemiro, F.; Fullarton, L.; Agwunobi, O.; Agbo, J.; Anowai, C.; Calvache, J.; van Vugt, N.; Gamezy, L.; Stainforth, J.;

Scientia Africana, Vol. 22 (No. 2), August, 2023. Pp 177-202
© Faculty of Science, University of Port Harcourt, Printed in Nigeria *ISSN 1118 – 1931*

Ganz, H.; Ladipo, K.; & F. Onichabor (2004). Regional Geological Framework Study of the Niger Delta, Resource Assessment and Geological Risking Volume 1: *Unpublished SPDC Document*.

Ekwenye, O.C. & O.C. Onyemesili (2020). A Review of the Heavy Mineral Provinces of the Paleogene Sediments, South-Eastern Nigeria: Factors Controlling the Distribution of the Heavy Minerals. *The Pacific Journal of Science and Technology*, 20(2), 289-300

Folk, R. L. & W.C. Ward (1957). Brazos River bar; a study in the significance of grain size parameters. *Journal of Sedimentary Petr*ology, 27, 3-27.

Friedman, G. M. (1979). Difference in the size distribution of populations of particles among sands of various origins. *Sedimentology*, 20, 3-32.

Friedman, G. M. & J.E. Sanders (1978). Principles of Sedimentology. John Wiley and Sons, New York.

Friedman, G. M. (1961). Distribution between dune, beach, and river sands from their textural characteristics. *Journal of Sedimentary Petr*ology, 31, 514-529.

Krumbein, W.C. & F.J. Pettijohn (1938). Manual of Sedimentary Petrography, Appleton Century Co, New York, 549p.

Ladipo, K. O. (1988). Paleogeography, sedimentation, and tectonics of the Upper Cretaceous Anambra Basin; South-eastern Nigeria. *Journal of African Earth Science*, 7(5) 865-869.

Murat, R. C. (1972). Stratigraphy and Paleogeography of the Cretaceous and Lower Tertiary in Southern Nigeria. In: T. F. J Dessauvagie, A. J. Whiteman (eds.), *African Geology*, Univ. of Ibadan Press, Nigeria, 251 -266.

Okoro, A. U. (1995). Petrology and depositional history of sandstone facies of the Nkporo Formation in the Leru area of south-eastern Nigeria. *Nigerian Journal of Mining Geology*, 105-112.

Oladotun, A.O. & O.A. Ehinola (2016). Hydrocarbon-charge modelling of Anambra basin, south-eastern Nigeria: implications for Cretaceous-sourced plays. *Arab Journal of Geoscience*, 9(171)

Passega, R. (1964). Grain size representation by C-M pattern: a geological tool. *Journal of Sedimentary Petr*ology 34, 831.

Petters, S. W. (1978). Stratigraphic evolution of the Benue Trough and its implication for the Upper Cretaceous paleogeography of West *African Journal of Geology*, 78, 311-322.

Pettijohn, F. J., 1975. Sedimentary Rocks. 3rd ed. Harper and Row, New York.

Reijers, T. J. A.; Petters, S. W. & C.S. Nwajide (1997). African Basins: In Selley, R. C. (ed.), *Sedimentary Basins of the World 3*, Elsevier Science B. V. Amsterdam, 151-172.

Reyment, R. A. (1965). Aspect of the Geology of Nigeria. Ibadan University Press, 145-153.

Sinclair, H. D. (1993). High-Resolution Stratigraphy and Facies differentiation of the Shallow marine Annot Sandstone, South-east France. *Journal of International Association of Sedimentologists*, 40(2)

Ugwueze, C.U., Ugwu S.A. & N.E. Ajaegwu (2019). Slope fan depositional elements evaluation: Implication for reservoir depositional origin in the deep offshore Niger Delta Basin, Nigeria, *Journal of African Earth Sciences, Elsevier*, Amsterdam, 160 (103638)

Ugwueze, C.U. and Ajaegwu, N.E., (2019). Tectonic Influence on Reservoir Quality Assessment of Deepwater Sandstones from the Offshore Niger Delta, Nigeria,

Journal of Basic Physical Research, 9(1) 13-24

Visher, G. S. (1969). Grain size distribution and depositional processes. *Journal of Sedimentary Petrology*, 39, 1074-1106.

Whiteman, A. J. (1982). Nigeria: its petroleum geology, resources, and potential. Graham and Trotman, London, 394.

Zarborski, P. M. P. (1983). Campano-Maastrichtian ammonites, correlation, and paleogeography in Nigeria. *Journal of African Earth Scienes*, 1, 59-63.

APPENDICES

Table 2a: Results of the Sieve Analysis from Leru Southwest

Sieve opening (mm)	Phi Scale (ϕ)	Weight (g)	Corrected weight(g)	Weight (%)	Cumulative weight (%)
> 4	< -2	0	0	0	0
4 - 2	-2 - -1	0.7	0.7	1.4	1.4
2 - 1	-1 - 0.0	3.6	3.6	7.2	8.6
1 - 0 .5	0.0 - 1	3.1	3.1	6.2	14.8
0.5 - 0.25	1 - 2	3.5	3.5	7	21.8
0.25 - 0.125	2 - 3	15.3	15.35	30.7	52.5
0.125 - 0.063	3 - 4	22.6	22.65	45.3	97.8
< 0.063	> 4	1.1	1.1	2.2	100
		= 49.9g	**= 50g**		

Original Sample Weight = 50g; Sieve Loss = 0.1g

Table 2b: Results of the Sieve Analysis from Leru Northwest

Sieve Opening (mm)	Phi Scale (ϕ)	Weight (g)	Corrected Weight (g)	Weight (%)	Cumulative Weight (%)
> 4	< -2	0.4	0.4	0.8	0.8
4 - 2	-2 - -1	1.7	1.72	3.44	4.24
2 - 1	-1 - 0.0	5.7	5.75	11.5	15.74
1 - 0 .5	0.0 - 1	7.1	7.17	14.34	30.08
0.5 - 0.25	1 - 2	23.7	23.79	47.58	77.66
0.25 - 0.125	2 - 3	10.1	10.17	20.34	98
0.125 - 0.063	3 - 4	1	1	2	100
		= 49.7g	**= 50g**		

Original Sample Weight = 50g; Sieve Loss = 0.3g

Table 2c: Results of the Sieve Analysis from Leru Northeast

Sieve Opening (mm)	Phi Scale (ϕ)	Weight (g)	Corrected Weight (g)	Weight (%)	Cumulative weight (%)
> 4	< -2	0	0	0	0
4 - 2	-2 - -1	0	0	0	0
2 - 1	-1 - 0.0	4	4	8	8
1 - 0 .5	0.0 - 1	16.35	16.35	32.7	40.7
0.5 - 0.25	1 - 2	24.95	24.95	49.9	90.6
0.25 - 0.125	2 - 3	4.2	4.2	8.4	99
0.125 -0.063	3 - 4	0.4	0.4	0.8	99.8
< 0.063	> 4	0.1	0.1	0.2	100
		= 50g	**= 50g**		

Original Sample Weight = 50g; Sieve Loss = 0.0g

Scientia Africana, Vol. 22 (No. 2), August, 2023. Pp 177-202
© Faculty of Science, University of Port Harcourt, Printed in Nigeria *ISSN 1118 – 1931*

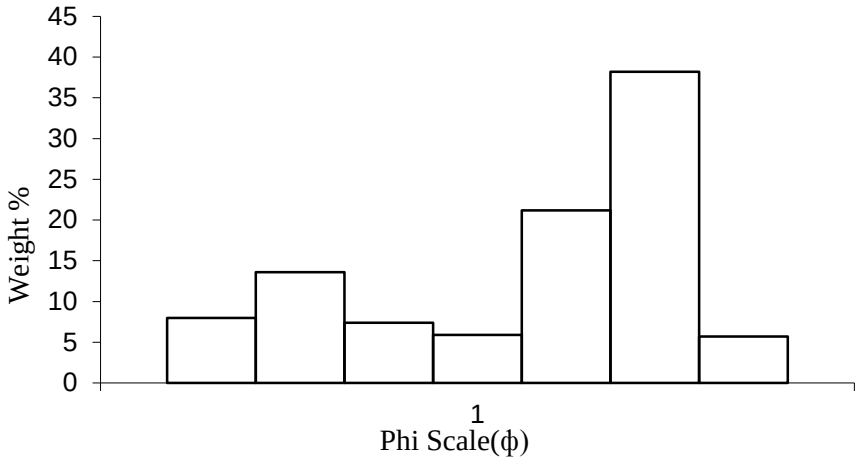

Fig. 6a: Histogram of Sandstones from the Leru Southwest

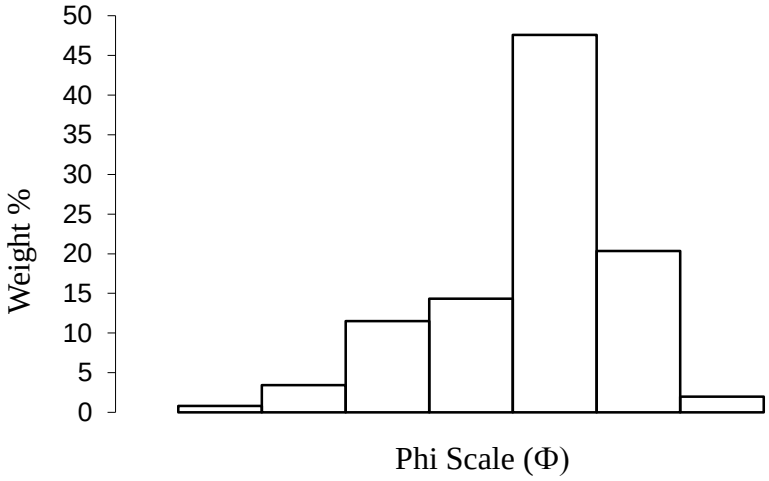

Fig. 6c: Histogram of Sandstones from the Leru Northwest

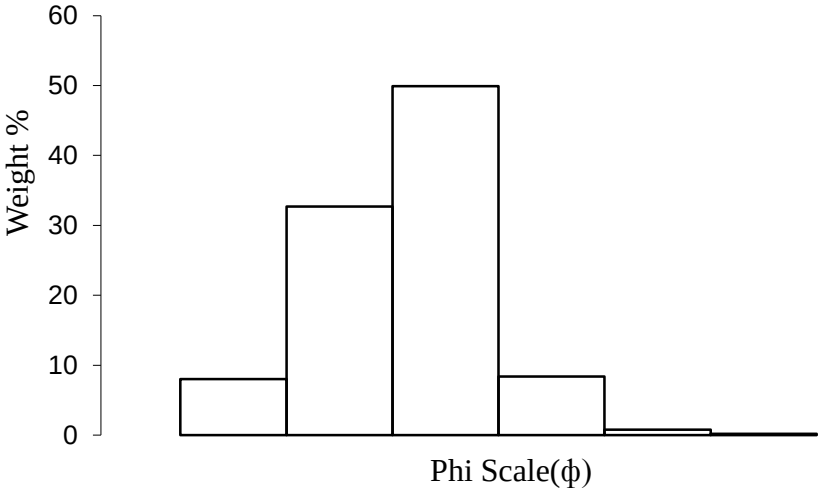

Fig. 6c: Histogram of Sandstones from the Leru Northeast

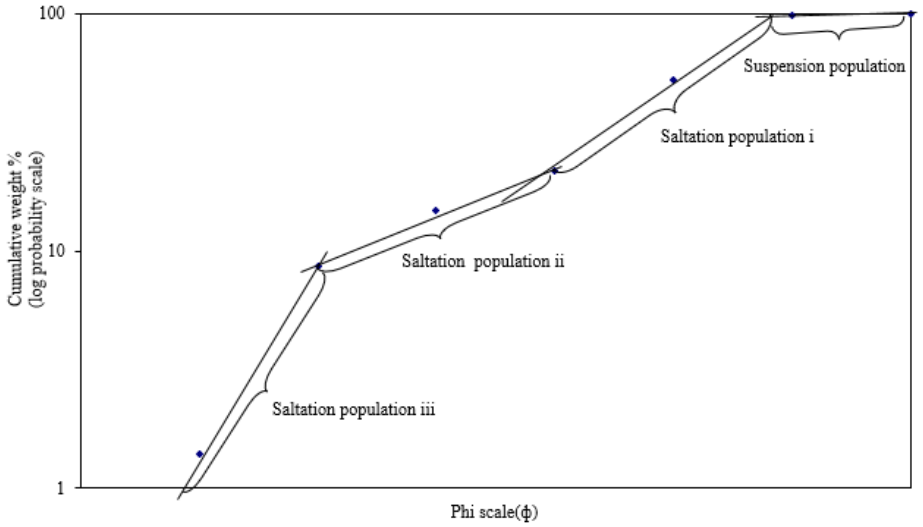

Fig 7a: Cumulative Log Probability Curve of Sandstones from the Leru Southwest

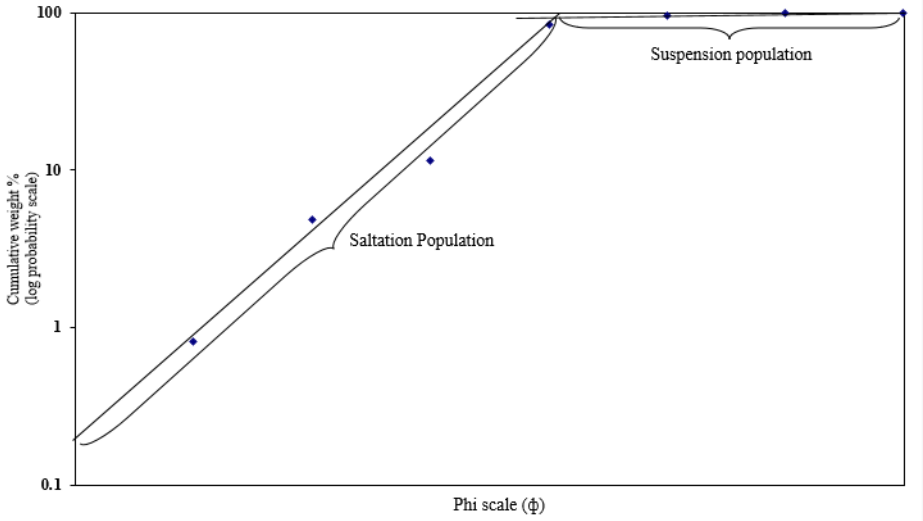

Fig 7b: Cumulative Log Probability Curve of Sandstones from the Leru Northwest

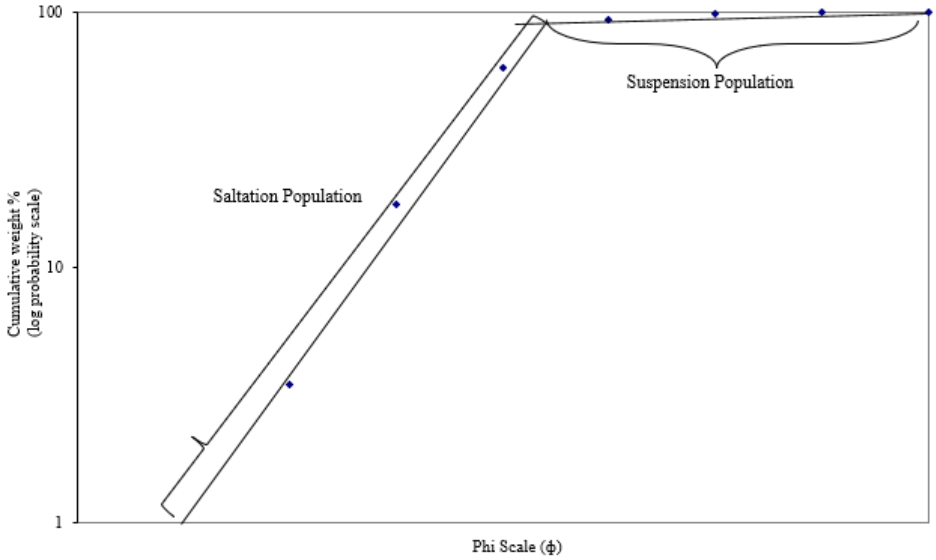

Fig 7c: Cumulative Log Probability Curve of Sandstones from the Leru Northeast

Scientia Africana, Vol. 22 (No. 2), August, 2023. Pp 177-202
© Faculty of Science, University of Port Harcourt, Printed in Nigeria *ISSN 1118 – 1931*

Table 3a: Results of the particle size distribution using statistical moments from Leru Southwest

(Φ)	**X_1**	**f**	**d = (x_1 - x_0)**	**fd**	**d^2**	**fd^2**	**d^3**	**fd^3**	**d^4**	**fd^4**
-2 - -1	-1.5	1.4	-5	-7	25	35	-125	-175	625	875
-1 - 0	-0.5	7.2	-4	-28.8	16	115.2	-64	-460.8	256	1843.2
0 - 1	0.5	6.2	-3	-18.6	9	55.8	-27	-167.4	81	502.2
1 - 2	1.5	7	-2	-14	4	28	-8	-56	16	112
2 - 3	2.5	30.7	-1	-30.7	1	30.7	-1	-30.7	1	30.7
3 - 4	3.5	45.3	0	0	0	0	0	0	0	0
4 - 5	4.5	2.2	1	2.2	1	2.2	1	2.2	1	2.2
		100		**-96.9**		**266.9**		**-887.7**		**3365.3**
		n = fd / 100		n_1 = -.969		n_2 = 2.67		n_3 = -8.88		n_4 = 33.65

(Φ) = Phi Scale

x1 = Midpoint of the grain diameter

f = Frequency of weight per cent

x0 = Midpoint of the grain diameter with the highest occurrence = **3.5**

d = (XI - X0) = Deviation, **d^2** = Deviation Squared, **d^3** = Cubed Deviation, **d^4** = Deviation Quadrupled

Table 3b: Results of the particle size distribution using statistical moments from Leru Northwest

(Φ)	**X_1**	**f**	**d = (x_1 - x_0)**	**fd**	**d^2**	**fd^2**	**d^3**	**fd^3**	**d^4**	**fd^4**
-2 - -1	-1.5	0.82	-3	-2.46	9	7.38	-27	-22.1	81	66.4
-1 - 0	-0.5	4.04	-2	-8.08	4	16.16	-8	-32.32	16	64.6
0 - 1	0.5	6.7	-1	-6.7	1	6.7	-1	-6.7	1	6.7
1 - 2	1.5	72.7	0	0	0	0	0	0	0	0
2 - 3	2.5	12.7	1	12.7	1	12.7	1	12.7	1	12.7
3 - 4	3.5	2.64	2	5.28	4	10.56	8	21.1	16	42.2
4 - 5	4.5	0.4	3	1.2	9	3.6	27	10.8	81	32.4
		100		**6.86**		**57.1**		**-16.5**		**225**
		n = fd / 100		**n_1 = .069**		**n_2 = .57**		**n_3 = -.165**		**n_4 = 2.25**

x0 = Midpoint of the grain diameter with the highest occurrence = **1.5**

Table 3c: Results of the particle size distribution using statistical moments from Leru Northeast

(Φ)	**X_1**	**f**	**d = (x_1 - x_0)**	**fd**	**d^2**	**fd^2**	**d^3**	**fd^3**	**d^4**	**fd^4**
-2 - -1	-1.5	1.24	-3	-3.7	9	11.2	-27	-33.5	81	100.4
-1 - 0	-0.5	9.8	-2	-19.6	4	39.2	-8	-78.4	16	156.8
0 - 1	0.5	25.8	-1	-25.8	1	25.8	-1	-25.8	1	25.8
1 - 2	1.5	55.2	0	0	0	0	0	0	0	0
2 - 3	2.5	6	1	6	1	6	1	6	1	6
3 - 4	3.5	1.26	2	2.5	4	5	8	10	16	20.2
4 - 5	4.5	0.7	3	2.1	9	6.3	27	18.9	81	56.7
		100		**-38.5**		**93.5**		**-102.7**		**366**
		n = fd / 100		**n_1 = -.39**		**n_2 = .94**		**n_3 = -1.03**		**n_4 = 3.66**

x0 = Midpoint of the grain diameter with the highest occurrence = **1.5**

Plate: 1: Massively bedded sandstones
Plate: 2: Massively bedded sandstones with little internal layering
Plate: 3: Heaved massive sandstones northwest section of the study area

Plate: 4: Thickly bedded argillaceous sandstones in the north-western part of the study area
Plate: 5: Tabular cross-bedded sandstones overlain by argillaceous sandstones

Scientia Africana, Vol. 22 (No. 2), August, 2023. Pp 177-202
© Faculty of Science, University of Port Harcourt, Printed in Nigeria *ISSN 1118 – 1931*

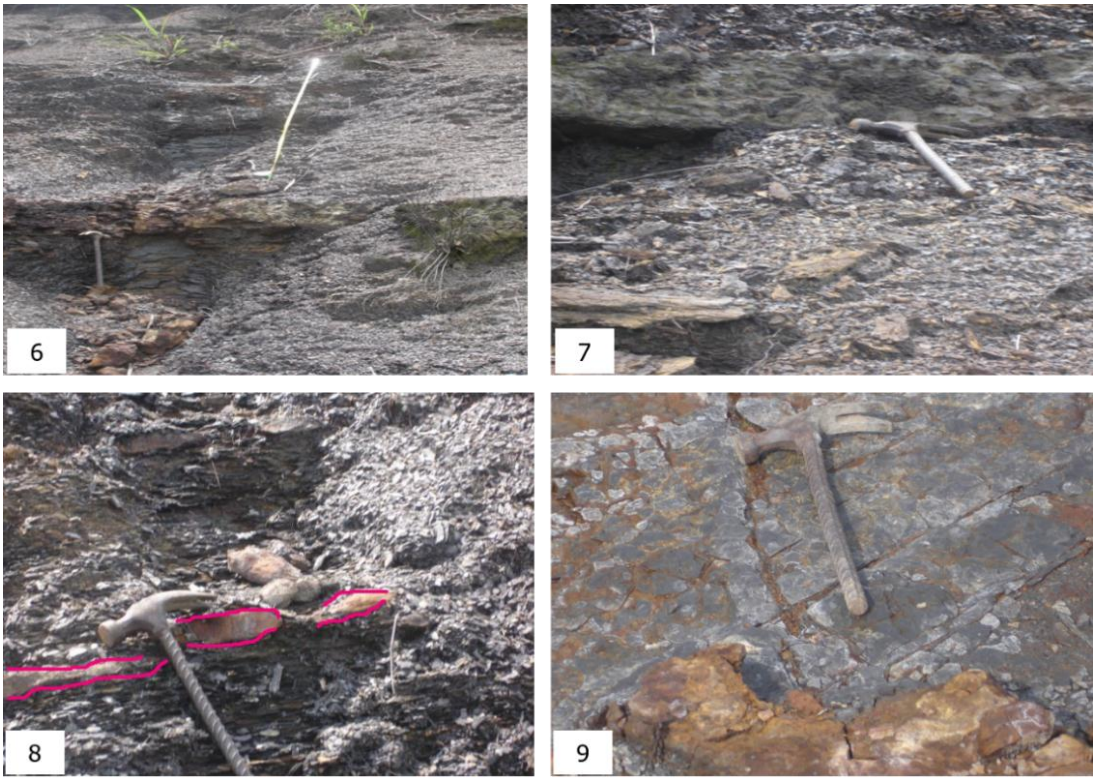

Plate: 6: Inter-bedded shale and mudstone sequence occurring within the central portion of the study area
Plate: 7: Weathered fissile black shales overlain by thick-bedded mudstone
Plate: 8: Nodular structures impregnated within the black shales
Plate: 9: Desiccation joints in clayey shale

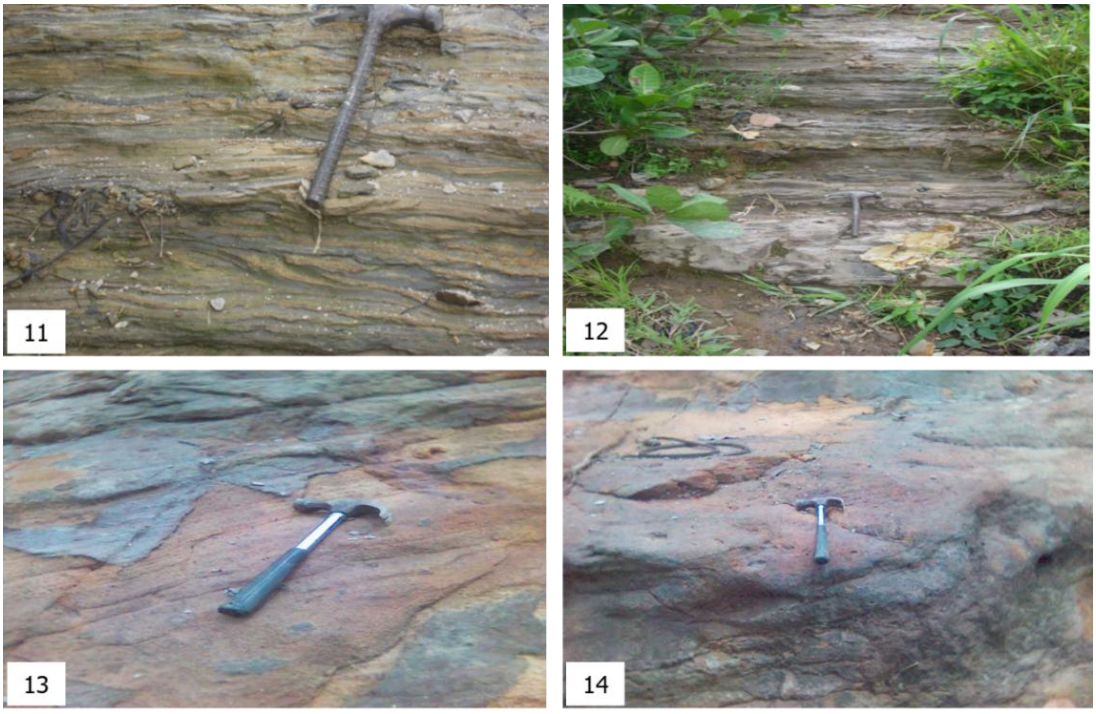

Plate: 11: Fine-grained ripple laminated sandstones with hummocky cross-stratification
Plate: 12: Inter-bedded planar and cross-bedded sandstones **SW** of the study area
Plate: 13: Planar cross-bedded sandstone facies overlying basal, large-scale cross-bedded sandstones
Plate: 14: Large-scale cross-bedded sandstones with few bioturbations **SE** of the study area

Plate: 15: Parallel laminated and flaky shales underlying large-scale cross-bedded sandstones **SW** of the study area
Plate: 16: Thin parallel laminated shales overlain by planar bedded argillaceous sandstones **NW** of the study area

Plate: 17: Vertically burrowed (Skolithos ichnofacies), coarse-grained sandstones **NE** of the study area
Plate: 18: Massive sandstones with rib joints **NE** of the study area